HHS Public Access

Author manuscript

Am J Surg Pathol. Author manuscript; available in PMC 2020 September 09.

Published in final edited form as:

Am J Surg Pathol. 2012 June ; 36(6): 857–868. doi:10.1097/PAS.0b013e31824644ac.

Malignant Gastrointestinal Neuroectodermal Tumor: Clinicopathologic, Immunohistochemical, Ultrastructural, and Molecular Analysis of 16 Cases With a Reappraisal of Clear Cell Sarcoma-like Tumors of the Gastrointestinal Tract

David L. Stockman, MD[*], **Markku Miettinen, MD**[†], **Saul Suster, MD**[*], **Dominic Spagnolo, MBBS, FRCPA, MD**[‡,§], **Hugo Dominguez-Malagon, MD**[‖], **Jason L. Hornick, MD, PhD**[¶], **Volkan Adsay, MD**[#], **Pauline M. Chou, MD, PhD**[**], **Benhur Amanuel, MBBS, FRCPA**[‡,§], **Peter VanTuinen, PhD**[*], **Eduardo V. Zambrano, MD**[*]

[*]Department of Pathology, The Medical College of Wisconsin, Milwaukee, WI

[†]Department of Soft Tissue Pathology, Armed Forces Institute of Pathology, Washington, DC

[‡]PathWest Laboratory Medicine WA

[§]School of PALM, University of Western Australia, Nedlands, WA, Australia

[‖]The National Cancer Institute of Mexico, Mexico City, Mexico

[¶]Department of Pathology, Brigham and Women's Hospital, Boston, MA

[#]Emory University Hospital, Atlanta, GA

[**]Children's Hospital Memorial Hospital, Chicago, IL.

Abstract

The clinical, histologic, immunophenotypic, ultrastructural, and molecular features of a distinctive gastrointestinal tumor are described. Sixteen patients, 8 women and 8 men aged 17 to 77 years (mean age, 42 y; 63% less than 40 y) presented with abdominal pain, intestinal obstruction, and an abdominal mass. Mean tumor size was 5.2 cm (range, 2.4 to 15.0 cm). The tumors arose in the small bowel (10), stomach (4), and colon (2) and were histologically characterized by a sheet-like or nested population of epithelioid or oval-to-spindle cells with small nucleoli and scattered mitoses. Five cases showed focal clearing of the cytoplasm. Scattered osteoclast-type multinucleated giant cells were present in 8 cases. The tumor cells were positive for S-100 protein, SOX10, and vimentin in 100% of cases, for CD56 in 70%, for synaptophysin in 56%, for NB84 in 50%, for NSE in 45%, and for neurofilament protein in 14% of cases. All cases tested were negative for specific melanocytic, gastrointestinal stromal tumors, epithelial, and myoid markers. Ultrastructural examination of 5 cases showed features of primitive neuroectodermal cells with clear secretory vesicles, dense-core granules, occasional gap junctions, and no evidence of melanogenesis. *EWSR1* gene rearrangement was assessed by fluorescence in situ hybridization in

Correspondence: Eduardo V. Zambrano, MD, Department of Pathology, Medical College of Wisconsin, 9200W. Wisconsin Ave., Milwaukee, WI 53226 (ezambrano@mcw.edu).

Conflicts of Interest and Source of Funding: The authors have disclosed that they have no significant relationships with, or financial interest in, any commercial companies pertaining to this article.

14 cases. Twelve cases (86%) showed split *EWSR1* signal consistent with a chromosomal translocation involving *EWSR1*. One case showed extra intact signals, indicating that the nuclei possessed either extra copies of the *EWSR1* gene or chromosome 22 polysomy. Only 1 case showed no involvement of the *EWSR1* gene. Six cases demonstrated rearrangement of the partner fusion gene *ATF1* (46%), and 3 showed rearrangement of *CREB1* (23%); 2 cases lacked rearrangement of either partner gene. Clinical follow-up was available in 12 patients and ranged from 1.5 to 106 months. Six patients died of their tumors (mean survival, 32 mo; 83% less than 24 mo). At last follow-up, 4 patients were alive with regional, lymph node, and liver metastases, and 2 patients were alive with no evidence of disease. The tumor described here is an aggressive form of neuroectodermal tumor that should be separated from other primitive epithelioid and spindle cell tumors of the gastrointestinal tract. The distinctive ultrastructural features and absence of melanocytic differentiation serve to separate them from soft tissue clear cell sarcomas involving the gastrointestinal tract. The designation “malignant gastrointestinal neuroectodermal tumor” is proposed for this tumor type.

Keywords

GNET; malignant gastrointestinal neuroectodermal tumor; clear cell sarcoma; gastrointestinal stromal tumor; neuroectodermal tumors; EWSR1; ATF1; CREB1; S-100 protein; GANT

Although most mesenchymal tumors of the gastrointestinal tract correspond to gastrointestinal stromal tumors (GIST), a small number of primary gastrointestinal tumors with features of clear cell sarcomas have been reported. Ekfors et al[14] identified a duodenal tumor displaying features similar to that of the clear cell sarcoma of tendons and aponeuroses (CCSTA), an entity originally described in 1965 by Enzinger and subsequently redesignated as “malignant melanoma of soft parts” in view of accumulating evidence of its melanocytic differentiation.[10] A distinctive chromosomal translocation involving *EWSR1-ATF1* t(12;22)(q13;q12) was noted in CCSTA by Bridge et al.[9] Because this distinctive chromosomal translocation is not present in cutaneous malignant melanomas,[25] CCSTA is currently considered a distinct entity separate from melanoma. A small number of cases arising in the gastrointestinal tract with similar morphologic, immunophenotypic, and molecular genetic features have now been reported.[1–3,6,7,11–14,16–18,21,22,24,26,27,31,34,36,38,40,41] However, many of these tumors have lacked evidence of melanocytic differentiation, and some authors have, therefore, preferred the designation “clear cell sarcoma-like tumor of the gastrointestinal tract” (CCSLTGT).[6,7,11,13,16,18,21–24,31,34,38,40,41]

We have reviewed 16 cases of gastrointestinal tumors displaying features similar to that of CCSLTGT. Our results indicate that these tumors, although sharing some features with CCSTA, differ in many significant respects and most likely represent a novel form of neuroectodermal tumor for which we propose the designation “malignant gastrointestinal neuroectodermal tumor” (GNET).

MATERIALS AND METHODS

The cases were retrieved from the surgical pathology and consult files of the Medical College of Wisconsin (Milwaukee, WI), the Armed Forces Institute of Pathology (Washington, DC), PathWest Laboratory Medicine WA (Nedlands, WA), Brigham and Women's Hospital (Boston, MA), Emory University Hospital (Atlanta, GA), and Children's Memorial Hospital (Chicago, IL) in the course of a retrospective review of clear cell sarcomas and mesenchymal tumors of the gastrointestinal tract accessioned at these institutions between 1976 and 2010. One case was previously published by the referring pathologist and subsequently reanalyzed for this study.[22] Hematoxylin and eosin-stained histological slides (1 to 36) were reviewed in all cases. Clinical information was obtained from referring physicians or from patient records. Cases with a history of melanoma or clear cell sarcoma of soft tissue were excluded. Inclusion criteria included primary gastrointestinal tumors composed of spindle-to-round or polygonal tumor cells arranged in sheets, fascicles, or nests, with immunohistochemical evidence of S-100 protein positivity but without expression of other immunohistochemical markers of melanocytic differentiation [Human melanoma black 45 (HMB45), melan A, and tyrosinase]. Representative paraffin blocks were available for immunohistochemical studies and for interphase fluorescence in situ hybridization (FISH) assay. This study was conducted in accordance with the regulations and with the approval of our institutional review board.

Immunohistochemistry

Immunohistochemical studies were conducted in selected formalin-fixed, paraffin-embedded blocks in all cases. A Dako autostainer using a standard avidin-biotin peroxidase complex technique (with blocking of endogenous biotin) was used for immunohistochemical studies. Heat-induced epitope retrieval was applied as pretreatment for selected markers. Diaminobenzidine was utilized as the chromogen. The primary antibodies have been summarized in Table 1. Appropriate positive and negative controls were run concurrently for all the markers tested.

Electron Microscopy

Five cases (nos 1 to 5) were examined by electron microscopy. In cases 1, 2, and 4, fresh tissue samples were diced into 1 mm^3 cubes, fixed in 2.5% glutaraldehyde, postfixed in osmium, embedded in EPON and routinely processed for transmission electron microscopy. Formalin-fixed, paraffin-embedded tissue samples in cases 3 and 5 were de-waxed, rehydrated, fixed in glutaraldehyde, and then processed for electron microscopy. Ultrathin sections from all EPON blocks were stained with uranyl acetate and lead citrate and examined in a JEOL 1010 TEM with a digital camera.

Molecular Studies

A total of 14 cases were examined for their cytogenetic profile. FISH for both *EWSR1* on chromosome 22q12 and for *FUS* on chromosome 16p11.2 was performed using the LSI *EWSR1* and LSI *FUS* dual-color, break-apart probes, respectively (Abbott Molecular, Des Plaines, IL), according to the manufacturer's recommendations. Tissue sections (4 mm thick) were placed onto slides, air-dried, and baked overnight at 601C. Slides were

deparaffinized in CitriSolv (Fisher, Vernon Hills, IL) 3 times for 7 minutes and then immersed twice in 100% ethanol for 3 minutes each. After air-drying, slides were pretreated with 1 M sodium thiocyanate for 30 minutes at 80°C, washed with dH_2O for 1 minute at 25°C, rinsed twice with 2× saline-sodium citrate (SSC) for 3 minutes at 25°C, and then dehydrated in 70%, 85%, and 100% ethanol and allowed to air-dry. Next, 10 to 20 μL of the dual-color break-apart probe (Abbott Molecular) was applied to the slides in an approximately 1 cm^2 area selected for a pure tumor population (> 90% tumor cells), and hybridization was performed at 37°C overnight in a moist chamber. Excess probe was washed away using 2X SSC/0.3% NP-40 (Fisher) at 731C for 2 minutes, and the nuclei were counterstained with 4′,6-diamidino-2-phenylindole dihydrochloride/DAPI II (Abbott Molecular).

FISH for rearrangement of *ATF1* on chromosome 12q13 was performed using centromeric clone RP11–831J22 (labeled with spectrum orange) and telomeric clone RP11–165G10 (labeled with spectrum green). FISH for *CREB1* on chromosome 2q34 was conducted using centromeric clone RP11–810D3 (labeled with spectrum orange) and telomeric clone RP11–361M16 (labeled with spectrum green). Paraffin sections were prepared for probe application using the same protocol as for the *EWSR1* probe. For both *ATF1* and *CREB1* probes, 1.5 μL of centromeric and telomeric probe DNA was mixed with 7.0 μL of hybridization solution (Abbott Molecular). Probes and slides were co-denatured at 80°C for 5 minutes and then hybridized at 37°C for 48 hours. Slides were immersed in prewarmed 0.4× SSC wash solution (72 ± 2°C) for 2 minutes, placed in 1X PBD at room temperature for 2 minutes, and then counterstained with 18 μL 4′,6-diamidino-2-phenylindole dihydrochloride/DAPI II (Abbott Molecular).

For scoring, the tissue sections were examined under an Olympus BX41 fluorescence microscope (Olympus) using a ×10 ocular and ×60 and ×100 oil immersion objectives. The slides were scanned, and the images were interpreted by a cytogeneticist (P.v.T.), who estimated the percentage of positive nuclei. Only cell nuclei with one or more yellow (fusion) and, in addition, separate green and red signals detected simultaneously were considered positive for *EWSR1* rearrangement. Signals were considered to be colocalized when their distance was equal to or smaller than the size of the hybridization signal. Negative controls were established on cultures of bone marrow aspirate specimens from known negative patients. Probe specificity was confirmed by mapping back to banded metaphase nuclei and by hybridization to previously identified cases with rearrangements involving 22q12 (*EWSR1*) on conventional cytogenetic and FISH analyses. This scoring method was used similarly for *FUS*, *CREB1*, and *ATF1* probes.

Samples were evaluated for the presence of fused or split signals in tumor cells, and an estimated percentage was reported. A positive result was reported when > 20% of tumor cells showed evidence of a rearrangement (split signal). A relatively high cutoff (above 5%) was set to allow more rigorous examination of cases falling within the 5% to 20% range; however, in practice this turned out to be unnecessary, as all of the positive cases showed > 50% rearrangements. When testing was uninterpretable in a sample, it was repeated once.

RESULTS

Clinical Findings

The clinicopathologic findings are summarized in Table 2. There were 8 women and 8 men aged 17 to 77 years (mean age, 42 y; 63% up to 40 y). Clinical signs and symptoms included abdominal pain, intestinal obstruction, or an abdominal mass discovered on imaging studies. Seven patients had liver metastases at the time of diagnosis, and 11 had lymph node metastases. Anorexia, anemia, weight loss, high-grade fever, and weakness were also reported. Clinical follow-up in 12 patients showed that 6 died of their tumors within 3 to 106 months after initial diagnosis (mean, 32 mo; 83% up to 24 mo). Four patients were alive with regional and liver metastases at 1.5 to 36 months, and 2 patients were alive with no evidence of disease at the time of last follow-up at 20 and 41 months. All tumors arose de novo without any history or evidence of a similar neoplasm in soft tissues or any other location; 10 cases were located in the small intestine (62.5%), 4 cases in the stomach (25%), and 2 in the colon (12.5%). Of the 10 cases arising in the small intestine, 4 occurred in the ileum and 3 in the jejunum.

Gross Features

The tumors ranged in size from 2.4 to 15 cm in greatest dimension (mean = 5.2 cm; median = 3.8 cm). The tumors were solid, firm, tan-white, and showed a lobulated cut surface with focal areas of hemorrhage and necrosis (Figs. 1A, B). A few of the tumors also showed focal cystic changes. Four tumors grew as exophytic, polypoid tumor nodules protruding into the bowel lumen. Four cases grew circumferentially, simulating a carcinoma. Nine tumors showed mucosal ulceration, and 8 displayed grossly transmural infiltration of the bowel wall.

Histologic Findings

The tumors were located primarily in the submucosa and muscularis propria, with occasional instances of mucosal involvement (Fig. 2A). Ulceration of the overlying mucosa was seen in 66% of cases. The majority of cases exhibited extensive areas of tumor necrosis. All tumors were characterized by a solid uniform neoplastic population composed of diffuse sheets or nests of epithelioid or oval-to-spindle tumor cells (Figs. 2B, C). The majority of tumor cells displayed a predominantly epithelioid appearance and contained round or oval nuclei surrounded by variable amounts of eosinophilic cytoplasm (Fig. 2D). The nuclei showed vesicular chromatin with peripheral margination, generally indistinct to small nucleoli, occasional prominent nucleoli, intranuclear cytoplasmic inclusions, and variable mitotic activity that ranged from 0 to 20 mitoses per 10HPF (mean, 6 mitoses per ten ×40 HPF). The tumors also focally displayed pseudoalveolar, pseudopapillary, microcystic, fascicular, and cord-like growth patterns (Figs. 3A, F). In 5 cases, focal clearing of the cytoplasm was present (Fig. 4A). Other areas showed a prominent fascicular spindle cell appearance (Fig. 4B). Scattered, unevenly distributed osteoclast-type giant cells were seen in 8 cases (Fig. 4C). Focal abortive rosette-like structures were seen in 6 cases (Fig. 4D), and patchy myxoid stromal change was observed in 4 cases. Recurrent or metastatic lesions showed morphology essentially similar to the original lesions, although some exhibited greater nuclear pleomorphism.

Immunohistochemical Findings

The results of immunohistochemical studies are presented in Table 3. All cases tested were S-100 protein (Fig. 5A), SOX10 (Fig. 5B), and vimentin positive. The majority displayed strong and diffuse nuclear and cytoplasmic positivity for S-100 protein; in 2 cases the staining was only focal. Melanocytic markers, HMB45, melan A, tyrosinase, and MiTF-M were negative in all the cases tested. Immunohistochemical markers associated with GIST, including DOG-1, CD34, and CD117, were negative. Neural and neuroendocrine markers including synaptophysin (Fig. 5C), CD56 (Fig. 5D), NB84, and neuron-specific enolase polyclonal were variably positive. CD56 was detected in 70% of cases (7/10), synaptophysin in 56% (9/16), NB84 in 50% (4/8), neuron-specific enolase polyclonal in 45% (5/11), and neurofilament protein in 14% (1/7) of cases. All cases assessed for NeuN, a marker of neuronal differentiation, were negative. Glial fibrillary acidic protein, desmin, α-smooth muscle actin, and CD99 were uniformly negative in all cases tested. All epithelial markers were also negative, except for 1 case showing some focal, spotty positivity for CAM5.2 (case 1). The proliferation marker (MIB-1) showed nuclear positivity ranging from 22% to 34% in all tested cases.

Ultrastructural Findings

Five cases were studied by electron microscopy, the results of which are shown in Table 4. Fresh, adequately fixed tissue was available in 3 cases. Two cases were retrieved from formalin-fixed paraffin-embedded tissue and showed suboptimal preservation. Ultrastructural examination disclosed sheets of polygonal cells with multiple interdigitating cell processes joined by macula adherenstype junctions. The cytoplasmic processes were slender or bulbous and contained dense-core secretory granules, clear secretory vesicles, few fine filaments, and scattered microtubules; synapse-like structures were often identified (Figs. 6A, B). In 1 case, cytoplasmic intermediate filaments (case 5) were seen. Case 2 comprised cells displaying both neuroaxonal and Schwannian-like features. None of the tumors studied showed evidence of myoid, melanocytic, or other specific type of differentiation.

Molecular Genetic Findings

Ewing sarcoma breakpoint region 1 gene (*EWSR1*) was studied in 14 cases by break-apart FISH. Twelve cases (86%) showed a split signal consistent with a chromosomal translocation involving *EWSR1* (Fig. 7A). One case (case 5) showed extra intact signals, indicating that the nuclei possessed either extra copies of the *EWSR1* gene or chromosome 22 polysomy. Involvement of the most common partner fusion genes, including those encoding cyclic adenosine monophosphate responsive binding protein 1 (*CREB1*) and activating transcription factor 1 (*ATF1*), were also studied by break-apart FISH. Of the 12 cases positive for a split *EWSR1* signal, 6 showed rearrangement of *ATF1* (50%) (Fig. 7B), 3 showed rearrangement of *CREB1* (25%), 2 showed no rearrangements of either *ATF1* or *CREB1* genes, and in 1 case *ATF1* and *CREB1* were not evaluated (case 16). One case showed no involvement of *EWSR1*, *ATF1*, or *CREB1* by FISH break-apart analysis (case 6). All 13 cases tested were negative for *FUS* gene rearrangement.

DISCUSSION

In recent years, gastrointestinal tumors bearing morphologic, immunohistochemical, and molecular features similar to the so-called CCSTA but without evidence of melanocytic differentiation have been described and designated as clear cell sarcomas and “clear cell sarcoma-like tumors of the gastrointestinal tract” (CCSLTGT).[1–3,6,7,11–14,16–18,21,22,24,26,27,31,34,36,38,40,41] Zambrano et al[41] initially proposed that a subset of these gastrointestinal tumors may correspond to a new, previously unrecognized entity. This was based on a report of 6 cases that lacked ultrastructural and immunophenotypic evidence of melanocytic differentiation while containing prominent osteoclast-type multinucleated giant cells and, in 2 of 3 cases examined ultrastructurally, the presence of dense-core secretory granules.

Review of the literature disclosed a total of 36 tumors reminiscent of CCSTA arising within the GI tract.[1–3,6,7,11–14,16–18,21,22,24,27,31,34,36,38,40,41] Twenty-four of them (including the 6 initially described by Zambrano and colleagues) showed diffuse S-100 protein positivity but absence of immunohistochemical or ultrastructural evidence for melanocytic differentiation.[6,7,11,13,16,18,21,22,24,31,34,38,40,41] The other 12 cases, however, showed immunophenotypic evidence of melanocytic differentiation.[1,2,12,14,17,27,36] From a review of the literature it appears that, in fact, there exist 2 distinct groups of tumors that, although exhibiting several similar features, differ in their realized lines of differentiation. Gastrointestinal tumors with features reminiscent of CCSTA but which show no specific evidence of melanocytic differentiation have been tentatively designated as “clear cell sarcoma-like tumors of the gastrointestinal tract” (CCSLTGT).

We have studied 16 cases of gastrointestinal tract neoplasms showing morphologic, ultrastructural, immunohistochemical, and molecular features similar to those seen in cases previously described as CCSLTGT. These tumors were positive for S-100 protein and SOX10 but lacked melanocyte-specific markers, including HMB45, melan A, tyrosinase, and microphthalmia transcription factor. Genetically, they were characterized by *EWSR1* gene rearrangements, including *EWSR1-ATF1* or *EWSR1-CREB1* fusions. At the ultrastructural level, they lacked evidence of melanocytic differentiation and showed features of neural differentiation, including multiple interdigitating cell processes containing dense-core granules and clear vesicles resembling synaptic bulbs. The features observed in these cases strongly suggest that such tumors may arise from an autonomic nervous system-related primitive cell of neural crest derivation that shows a neural line of differentiation with complete absence of melanocytic features. We conclude that these tumors comprise a distinct clinicopathologic entity, which we propose to designate as “malignant gastrointestinal neuroectodermal tumor” (GNET).

The tumors described herein occur mainly in young-aged to middle-aged adults and occasionally in older patients. They represent a highly malignant neoplasm with poor prognosis. Six of 12 patients with follow-up information died of their tumors (mean survival, 32 mo), and 4 additional patients were alive with regional, lymph node, and liver metastases.

Histologically, GNET is characterized by sheets or nests of primitive epithelioid-to-oval or occasionally spindle tumor cells. Osteoclast-type giant cells are a common feature (50% of cases). The immunohistochemical profile is suggestive of a primitive neural phenotype (positivity for S-100 protein, SOX10, NSE, synaptophysin, CD56, and NB84), without expression of melanocytic markers (HMB45, melan A, tyrosinase, and microphthalmia transcription factor). Similar evidence for a primitive neural phenotype was also recognized by Antonescu et al[6] in their study of 3 cases of CCSLTGT. They suggested that these tumors possibly arose from a gastrointestinal neuroectodermal precursor cell that had lost the potential to differentiate along the melanocytic lineage. Ultrastructural analysis also shows evidence of neural differentiation in these tumors, including interdigitating cell processes containing bulbous dilatations and dense-core granules consistent with synaptic bulbs, and absence of melanosomes. It is of interest that similar ultrastructural features, including the presence of dense-core or electron-dense granules as well as “melanosome-like structures” that probably represented abnormal or abortive dense-core granules, have also been described in previously reported tumors in cases that showed no immunohistochemical evidence of melanocytic differentiation.[3,6,13,31]

The molecular genetic study in 13 of our cases showed *EWSR1* gene rearrangements, usually fused with *ATF1* or *CREB1*, a finding that is shared with several other types of tumors of uncertain or disputed histogenesis.[4,5,20,30,33,35] The *EWSR1* gene product is a member of the TET family of transcription factors. Rearrangements of this gene occur in Ewing sarcoma, hyalinizing clear cell carcinoma of salivary gland,[5] myoepithelial carcinoma,[15] extraskeletal myxoid chondrosarcoma, myxoid liposarcoma, angiomatoid fibrous histiocytoma, and desmoplastic small round cell tumors.[37] The fusion translocation *EWSR1-ATF1* has been noted in CCSTA,[9] hyalinizing clear cell carcinoma of salivary gland,[5] polyphenotypical round cell sarcoma of bone,[35] and in angiomatoid fibrous histiocytoma.[4,20,33] The fusion translocation *EWSR1-CREB1* has been identified in CCSTA, angiomatoid fibrous histiocytoma,[4] primary pulmonary myxoid sarcoma,[39] and small blue round cell tumor of the interosseous membrane.[30] As pointed out by Barr and Zhang,[8] the fact that some tumors share common molecular rearrangements with other related and unrelated neoplasms may be indicative of the fact that the different phenotypes are not the direct result of the genetic fusion subtype but rather of the stage of maturation or differentiation of the precursor cells in which the chimeric gene is being expressed. As more of these molecular and genetic abnormalities are discovered, it becomes increasingly apparent that genetic rearrangements should not be regarded as being necessarily diagnostic or pathognomonic of specific neoplastic entities in isolation of other findings, as has been evidenced by other examples of molecular promiscuity in other clinically and morphologically unrelated tumors.[37] The different phenotypes and clinical behavior of these various entities that share the same genetic alteration may be explained on the basis of the different milieu surrounding the affected progenitor tumor cells. Alternatively, they could be the consequence of the various differentiation programs already present in the progenitor tumor cells in which these genetic events occur. The genetic alteration involving the *EWSR1* gene in our cases may thus be an expression of close genetic kinship with other similar tumors harboring similar translocations but may not serve to define nosologically a specific

tumor entity or be regarded as indicative of exact homology with other tumors bearing a similar molecular abnormality, such as CCSTA.

According to our results, alternative molecular pathways involving additional unidentified genes may also be associated with the development of these neoplasms, even in the absence of rearrangements involving *EWSR1*, *ATF1*, and *CREB1*. *FUS* (fused in sarcoma, 16p11.2), a gene that shares extensive nucleotide sequence homology with *EWSR1*, has been identified as an alternative partner gene to *EWSR1* in certain tumors, including angiomatoid fibrous histiocytoma and myxoid liposarcoma.[32] For this reason, we hypothesized that *FUS* may be involved in some cases of GNET when *EWSR1* is not rearranged. However, none of the cases analyzed in our study showed rearrangements involving *FUS*, including 1 case negative for *EWSR1*, *ATF1*, and *CREB1* rearrangements.

The differential diagnosis for GNET includes GIST, monophasic synovial sarcoma, primary or metastatic malignant melanoma, and CCSTA. Distinguishing GNET from other sarcomas of the gastrointestinal tract, especially GIST, is important because of their different pathogenesis and response to treatment.

The most difficult differential diagnosis lies with CCSTA involving the gastrointestinal tract (“true” clear cell sarcoma). Because of their similar histologic appearance, S-100 protein expression, and shared molecular translocations, separating the 2 will require a more detailed immunohistochemical analysis utilizing specific melanocytic-associated markers and, in equivocal cases, electron microscopy to demonstrate the total lack of melanocytic features and evidence of neural differentiation in the tumor cells.

Because of its intramural location in the gastrointestinal tract and its histologic features, GIST also enters the differential diagnosis. As in our tumors, GISTs are also characterized by spindle and epithelial cells, making their distinction extremely difficult on the basis of morphology alone. Immunohistochemistry can reliably distinguish these 2 entities, as all GIST markers [CD117 (c-kit), DOG-1, and CD34] were universally negative in all of our cases. The possibility of a kit-negative GIST also needs to be considered; however, such tumors usually display DOG-1 and/or CD34 positivity.[29]

A few rare cases of monophasic synovial sarcoma arising in the wall of the gastrointestinal tract have also been described in the literature.[28] The tumors can histologically closely resemble GNET and may be very difficult to distinguish from our cases on the basis of morphology alone. Immunohistochemical stains will be of value in this setting by showing lack of staining for epithelial markers in GNET. Because S-100 protein has been observed in up to 30% of synovial sarcomas of soft tissue,[19] epithelial markers should always be included when investigating the possibility of GNET. Equivocal cases should be further evaluated for translocations. Synovial sarcoma is characterized by the *SYT* rearrangement in t(X;18), unlike GNET, which will demonstrate rearrangements of *EWSR1*.

In short, GNET should be suspected in any tumor arising in the wall of the gastrointestinal tract displaying an epithelioid or spindle cell population with S-100 protein positivity and lacking any specific markers of melanocytic differentiation. This should prompt a molecular study to confirm involvement of *EWSR1* chromosomal rearrangement with the

corresponding fusion partner genes. In equivocal cases, ultrastructural examination can be of additional help for the differential diagnosis. A combined approach utilizing immunohistochemistry and ultrastructural and molecular analyses is recommended for proper identification of these tumors and for separating them from their mimics.

REFERENCES

1. Abdulkader I, Cameselle-Teijeiro J, de Alava E, et al. Intestinal clear cell sarcoma with melanocytic differentiation and EWS [corrected] rearrangement: report of a case. Int J Surg Pathol. 2008; 16:189–193. [PubMed: 18417679]
2. Achten R, Debiec-Rychter M, De Wever I, et al. An unusual case of clear cell sarcoma arising in the jejunum highlights the diagnostic value of molecular genetic techniques in establishing a correct diagnosis. Histopathology. 2005;46:472–474. [PubMed: 15810965]
3. Alpers CE, Beckstead JH. Malignant neuroendocrine tumor of the jejunum with osteoclast-like giant cells. Enzyme histochemistry distinguishes tumor cells from giant cells. Am J Surg Pathol. 1985;9: 57–64. [PubMed: 2578748]
4. Antonescu CR, Dal Cin P, Nafa K, et al. EWSR1-CREB1 is the predominant gene fusion in angiomatoid fibrous histiocytoma. Genes Chromosomes Cancer. 2007;46:1051–1060. [PubMed: 17724745]
5. Antonescu CR, Katabi N, Zhang L, et al. EWSR1-ATF1 fusion is a novel and consistent finding in hyalinizing clear-cell carcinoma of salivary gland. Genes Chromosomes Cancer. 2011;50: 559–570. [PubMed: 21484932]
6. Antonescu CR, Nafa K, Segal NH, et al. EWS-CREB1: a recurrent variant fusion in clear cell sarcoma—association with gastrointestinal location and absence of melanocytic differentiation. Clin Cancer Res. 2006;12:5356–5362. [PubMed: 17000668]
7. Balkaransingh P, Saad SA, Govil SC, et al. Clear cell sarcoma of the gastrointestinal tract presenting as a second malignant neoplasm following neuroblastoma in infancy. Pediatr Blood Cancer. 2011 [Epub ahead of print].
8. Barr FG, Zhang PJ. The impact of genetics on sarcoma diagnosis: an evolving science. Clin Cancer Res. 2006;12:5256–5257. [PubMed: 17000654]
9. Bridge JA, Borek DA, Neff JR, et al. Chromosomal abnormalities in clear cell sarcoma. Implications for histogenesis. Am J Clin Pathol. 1990;93:26–31. [PubMed: 2294702]
10. Chung EB, Enzinger FM. Malignant melanoma of soft parts. A reassessment of clear cell sarcoma. Am J Surg Pathol. 1983;7: 405–413. [PubMed: 6614306]
11. Comin CE, Novelli L, Tornaboni D, et al. Clear cell sarcoma of the ileum: report of a case and review of literature. Virchows Arch. 2007;451:839–845. [PubMed: 17636326]
12. Covinsky M, Gong S, Rajaram V, et al. EWS-ATF1 fusion transcripts in gastrointestinal tumors previously diagnosed as malignant melanoma. Hum Pathol. 2005;36:74–81. [PubMed: 15712185]
13. Donner LR, Trompler RA, Dobin S. Clear cell sarcoma of the ileum: the crucial role of cytogenetics for the diagnosis. Am J Surg Pathol. 1998;22:121–124. [PubMed: 9422325]
14. Ekfors TO, Kujari H, Isomaki M. Clear cell sarcoma of tendons and aponeuroses (malignant melanoma of soft parts) in the duodenum: the first visceral case. Histopathology. 1993;22:255–259. [PubMed: 7684355]
15. El-Kabany M, Al-Abdulghani R, Ali AE, et al. Soft tissue high grade myoepithelial carcinoma with round cell morphology: report of a newly described entity with EWSR1 gene rearrangement. Gulf J Oncolog. 2011;1:73–77.
16. Friedrichs N, Testi MA, Moiraghi L, et al. Clear cell sarcoma-like tumor with osteoclast-like giant cells in the small bowel: further evidence for a new tumor entity. Int J Surg Pathol. 2005;13:313–318. [PubMed: 16273186]
17. Fukuda T, Kakihara T, Baba K, et al. Clear cell sarcoma arising in the transverse colon. Pathol Int. 2000;50:412–416. [PubMed: 10849331]
18. Granville L, Hicks J, Popek E, et al. Visceral clear cell sarcoma of soft tissue with confirmation by EWS-ATF1 fusion detection. Ultrastruct Pathol. 2006;30:111–118. [PubMed: 16517477]

19. Guillou LWC, Kraus MD, Dei Tos AP. Fletcher CDM. S-100 protein reactivity in synovial sarcomas—a potentially frequent diagnostic pitfall. Immunohistochemical analysis of 100 cases. Appl Immunohistochem Mol Morphol. 1996;4:167–175.
20. Hallor KH, Mertens F, Jin Y, et al. Fusion of the EWSR1 and ATF1 genes without expression of the MITF-M transcript in angiomatoid fibrous histiocytoma. Genes Chromosomes Cancer. 2005;44:97–102. [PubMed: 15884099]
21. Huang W, Zhang X, Li D, et al. Osteoclast-rich tumor of the gastrointestinal tract with features resembling those of clear cell sarcoma of soft parts. Virchows Arch. 2006;448:200–203. [PubMed: 16220298]
22. Joo M, Chang SH, Kim H, et al. Primary gastrointestinal clear cell sarcoma: report of 2 cases, one case associated with IgG4-related sclerosing disease, and review of literature. Ann Diagn Pathol. 2009;13:30–35. [PubMed: 19118779]
23. Kosemehmetoglu K, Folpe AL. Clear cell sarcoma of tendons and aponeuroses, and osteoclast-rich tumour of the gastrointestinal tract with features resembling clear cell sarcoma of soft parts: a review and update. J Clin Pathol. 2010;63:416–423. [PubMed: 20418233]
24. Lagmay JP, Ranalli M, Arcila M, et al. Clear cell sarcoma of the stomach. Pediatr Blood Cancer. 2009;53:214–216. [PubMed: 19350639]
25. Langezaal SM, Graadt van Roggen JF, Cleton-Jansen AM, et al. Malignant melanoma is genetically distinct from clear cell sarcoma of tendons and aponeurosis (malignant melanoma of soft parts). Br J Cancer. 2001;84:535–538. [PubMed: 11207050]
26. Leung KM, Wong S, Chow TC, et al. A malignant gastrointestinal stromal tumor with osteoclast-like giant cells. Arch Pathol Lab Med. 2002;126:972–974. [PubMed: 12171499]
27. Lyle PL, Amato CM, Fitzpatrick JE, et al. Gastrointestinal melanoma or clear cell sarcoma? Molecular evaluation of 7 cases previously diagnosed as malignant melanoma. Am J Surg Pathol. 2008;32:858–866. [PubMed: 18408594]
28. Makhlouf HR, Ahrens W, Agarwal B, et al. Synovial sarcoma of the stomach: a clinicopathologic, immunohistochemical, and molecular genetic study of 10 cases. Am J Surg Pathol. 2008;32: 275–281. [PubMed: 18223331]
29. Miettinen M, Wang ZF, Lasota J. DOG1 antibody in the differential diagnosis of gastrointestinal stromal tumors: a study of 1840 cases. Am J Surg Pathol. 2009;33:1401–1408. [PubMed: 19606013]
30. Pacheco M, Horsman DE, Hayes MM, et al. Small blue round cell tumor of the interosseous membrane bearing a t(2;22)(q34;q12)/EWS-CREB1 translocation: a case report. Mol Cytogenet. 2010; 3:12. [PubMed: 20598147]
31. Pauwels P, Debiec-Rychter M, Sciot R, et al. Clear cell sarcoma of the stomach. Histopathology. 2002;41:526–530. [PubMed: 12460205]
32. Raddaoui E, Donner LR, Panagopoulos I. Fusion of the FUS and ATF1 genes in a large, deep-seated angiomatoid fibrous histiocytoma. Diagn Mol Pathol. 2002;11:157–162. [PubMed: 12218455]
33. Rossi S, Szuhai K, Ijszenga M, et al. EWSR1-CREB1 and EWSR1-ATF1 fusion genes in angiomatoid fibrous histiocytoma. Clin Cancer Res. 2007;13:7322–7328. [PubMed: 18094413]
34. Shenjere P, Salman WD, Singh M, et al. Intra-abdominal clear-cell sarcoma: a report of 3 cases, including 1 case with unusual morphological features, and review of the literature. Int J Surg Pathol. 2011 [Epub ahead of print].
35. Somers GR, Viero S, Nathan PC, et al. Association of the t(12;22)(q13;q12) EWS/ATF1 rearrangement with polyphenotypic round cell sarcoma of bone: a case report. Am J Surg Pathol. 2005; 29:1673–1679. [PubMed: 16327442]
36. Taminelli L, Zaman K, Gengler C, et al. Primary clear cell sarcoma of the ileum: an uncommon and misleading site. Virchows Arch. 2005;447:772–777. [PubMed: 16021514]
37. Tanas MR, Rubin BP, Tubbs RR, et al. Utilization of fluorescence in situ hybridization in the diagnosis of 230 mesenchymal neoplasms: an institutional experience. Arch Pathol Lab Med. 2010;134: 1797–1803. [PubMed: 21128778]

38. Terazawa K, Otsuka H, Morita N, et al. Clear-cell sarcoma of the small intestine detected by FDG-PET/CT during comprehensive examination of an inflammatory reaction. J Med Invest. 2009;56: 70–75. [PubMed: 19262017]

39. Thway K, Nicholson AG, Lawson K, et al. Primary pulmonary myxoid sarcoma with EWSR1-CREB1 fusion: a new tumor entity. Am J Surg Pathol. 2011;35:1722–1732. [PubMed: 21997693]

40. Venkataraman G, Quinn AM, Williams J, et al. Clear cell sarcoma of the small bowel: a potential pitfall. Case report. APMIS. 2005;113:716–719. [PubMed: 16309433]

41. Zambrano E, Reyes-Mugica M, Franchi A, et al. An osteoclast-rich tumor of the gastrointestinal tract with features resembling clear cell sarcoma of soft parts: reports of 6 cases of a GIST simulator. Int J Surg Pathol. 2003;11:75–81. [PubMed: 12754623]

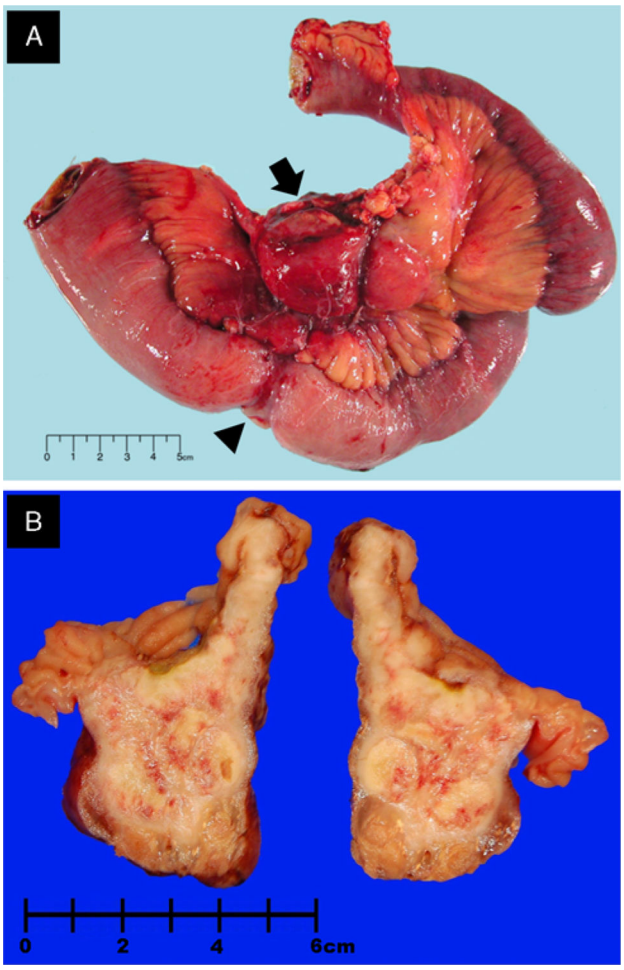

FIGURE 1.

Gross photographs. A, Annular mass (case 3) (arrowhead) involving full thickness of the ileal wall with mesenteric extension (arrow). B, Cut section of the small bowel with an intramural nodular mass (case 1).

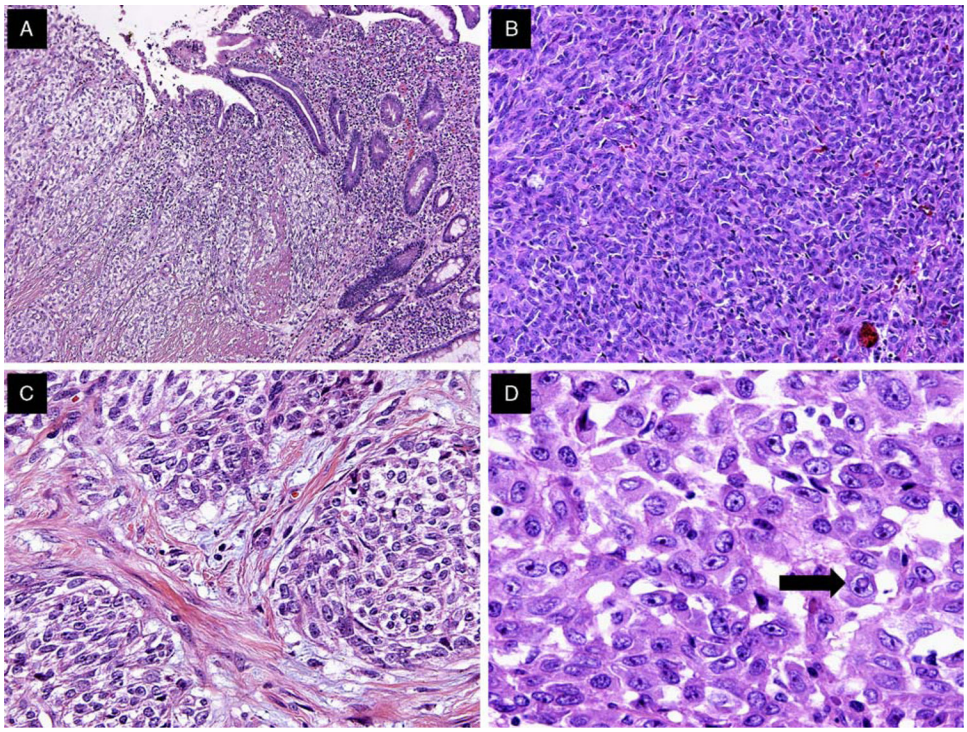

FIGURE 2.

Predominant histomorphologic and cytologic features of GNET. A, GNET involvement of the bowel wall and mucosal invasion with tumor cells infiltrating the lamina propria. B, GNET with a predominant solid pattern; note the lack of clear cell morphology. C, GNET with occasional melanoma-like nesting pattern and clear cell features. D, High magnification of typical GNET cytology. Cells are epithelioid and polygonal with eosinophilic cytoplasm. Pleomorphic nuclei showed vesicular chromatin, prominent nucleoli, and occasional intranuclear cytoplasmic inclusions (arrow).

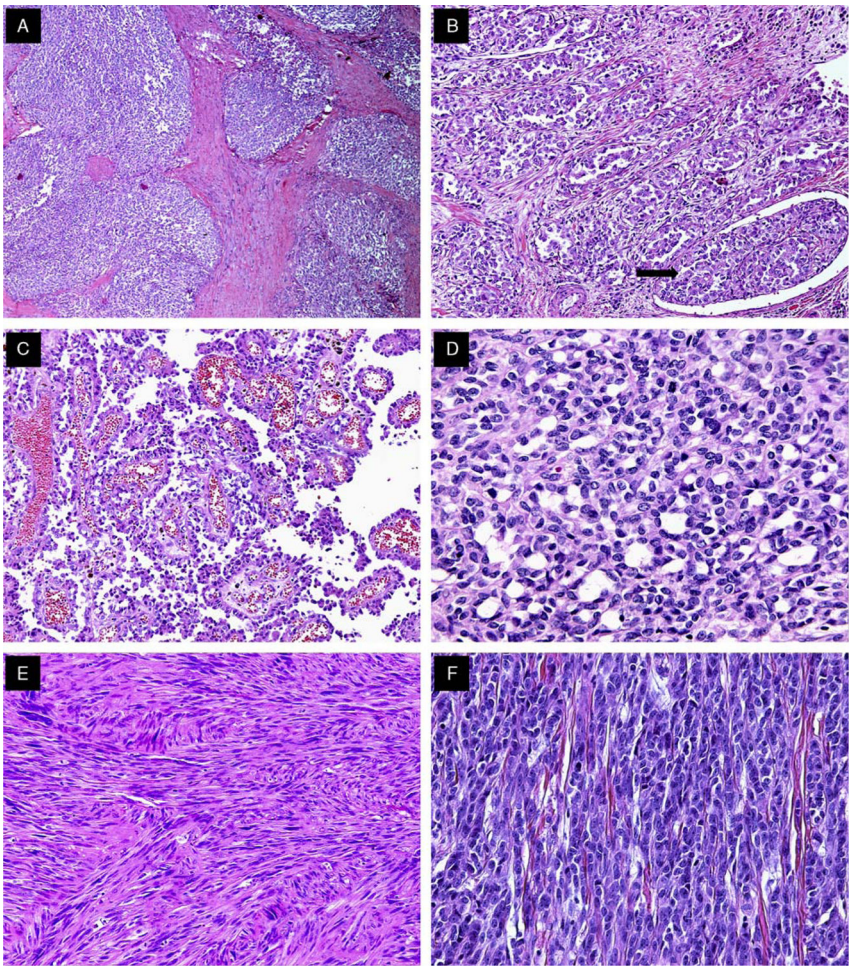

FIGURE 3.

Histologic spectrum of GNET. A, Low magnification of a GNET displaying nested architecture. B, GNET with occasional areas displaying pseudoalveolar pattern. Note the focus of lymphovascular invasion (arrow) (case 3). C, GNET with pseudopapillary architecture (case 3). D, Focal microcystic areas of GNET (case 6). E, Spindle cell GNET displaying fascicular architectural pattern (case 5). F, GNET with occasional areas of cord-like growth.

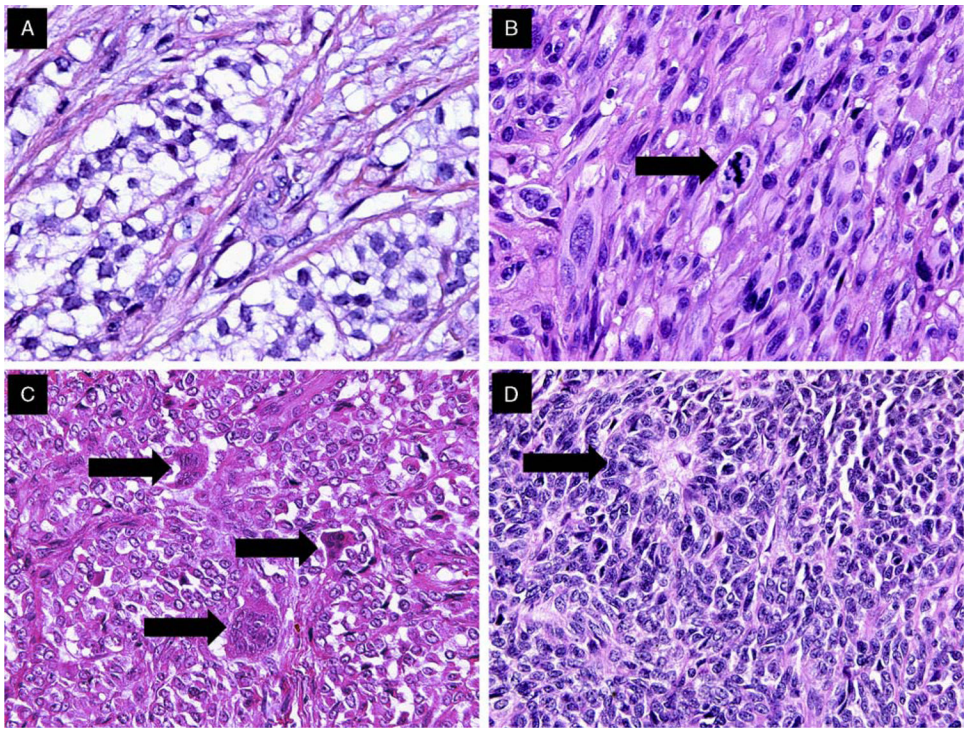

FIGURE 4.

Examples of histologic features of GNETs. A, Focal clearing of the cytoplasm was relatively uncommon. B, Admixed spindle and epithelioid tumor cells; mitosis (arrow). C, Multinucleated osteoclast-like giant cells (arrows), were observed in half of the cases. D, Occasional rosette-like structures (arrow) were identified in several cases.

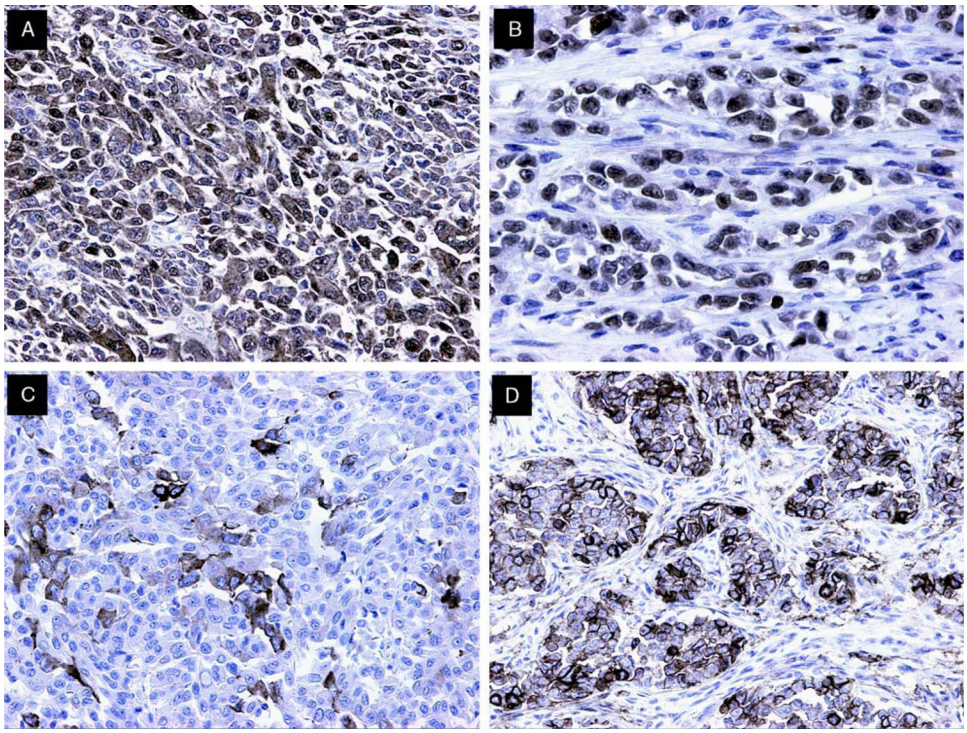

FIGURE 5.

Immunohistochemical findings in GNET. A, S-100 protein expression was mainly strong and diffuse, in a nuclear and cytoplasmic distribution. B, SOX10 staining was uniformly strongly positive in the majority of tumor cells. C, Synaptophysin expression was common, with most cases displaying focal but strong cytoplasmic staining. D, CD56 expression was variable. Note staining of neoplastic cells arranged in nests surrounded by desmoplastic stroma.

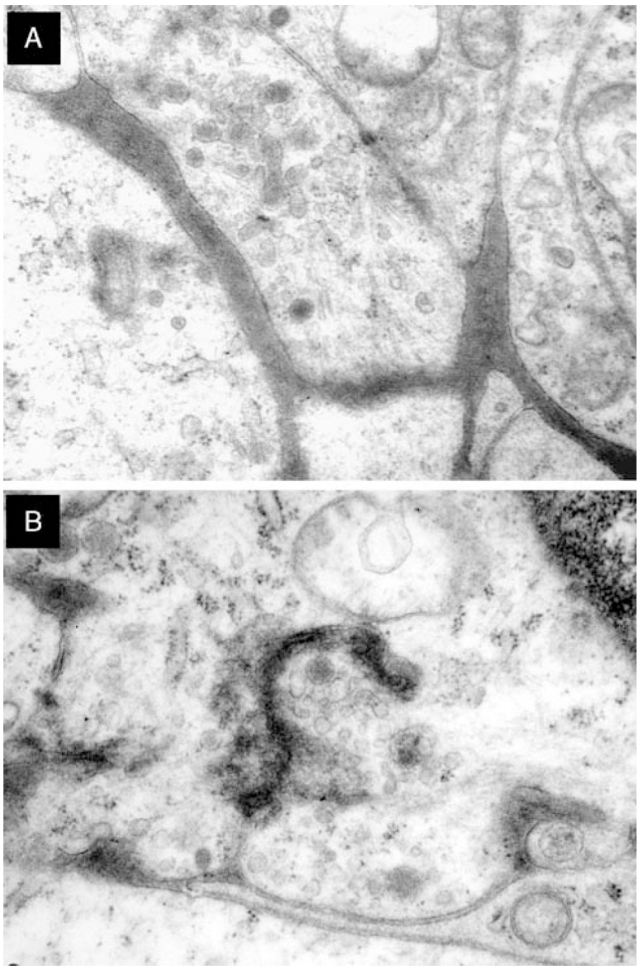

FIGURE 6.

Ultrastructural features of GNET. A, Cell processes containing secretory dense-core granules, clear vesicles, sparse filaments, and few microtubules. B, Synapse-like structure showing a gap junction between 2 cytoplasmic processes (case 2). Clear vesicles concentrated near the junction; there are isolated dense-core secretory granules; scattered microtubules and ill-defined filaments may be discerned.

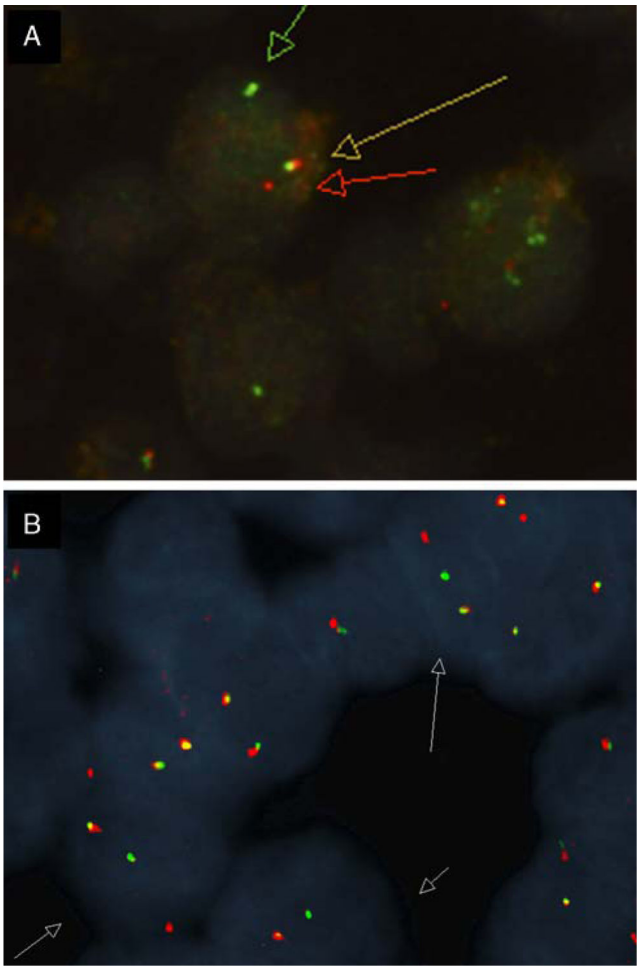

FIGURE 7.
FISH studies. A, *EWSR1* showing split-apart signals in the neoplastic cells. B, *ATF1* showing split-apart signals in the neoplastic cells (case 2).

TABLE 1.

Antibodies, Sources, and Dilutions

Antibody	Source	Clone	Antibody Dilution
AE1/AE3	Dako (Carpinteria, CA)	AE1/AE3	1:300
Cam 5.2	BD Biosciences (San Jose, CA)	CAM 5.2	1:50
CD34	Dako	QBEnd10	1:400
CD56	Vector (Burlingame, CA)	CD564	1:100
CD99	Covance Inc. (Princeton, NJ)	O13	1:400
CD117 (c-kit)	Zymed (Camarillo, CA)	2E4	1:150
Chromogranin A	Dako	DAK-A3	1:3000
Desmin	Dako	D33	1:75
DOG-1	Novacastra (Newcastle, UK)	K9	1:200
GFAP	Dako	6F2	1:200
HMB45	Leica Microsystems Inc. (Bannockburn, IL)	HMB45	1:30
Ki-67	Dako	MIB-1	1:75
Melan A	Dako	A103	1:100
MiTF-M	Cell Marque Corp. (Rocklin, CA)	C5/D5	1:300
NB84	Leica Microsystems Inc.	NB84	1:100
Neurofilament protein	Dako	2F11	1:100
NeuN	Millipore Corporation (Billerica, MA)	A60	1:100
Neuron-specific enolase	Covance Inc.	NSE-P1	1:150
S-100	Cell Marque Corp.	4C4.9	1:750
Smooth muscle actin	Dako	1A4	1:500
SOX10	R&D Systems Inc. (Minneapolis, MN)	20B7	1:500
Synaptophysin	Cell Marque Corp.	SY38	1:300
Tyrosinase	Cell Marque Corp.	T311	1:50
Vimentin	Dako	VimB4	1:400

DOG-1 indicates discovered on GIST 1; GFAP, glial fibrillary acidic protein.

TABLE 2.

Summary of Clinicopathologic Features of GNET

Case	Molecular Studies	A/S	Location	Morphology	Growth Pattern	OLGC	S-100	SOX10	Synaptophysin	CD56	NB84	NSE-p	Follow-up
1	*EWSR1-ATF1*	30/F	Jejunum	Epithelioid	Solid sheets, nests	−	+++	+++	++	+	+	++	AWD at 21 mo
2	*EWSR1-ATF1*	35/M	Jejunum	Epithelioid, oval	Solid sheets, nests	+	+++	+++	+	+	+	+	DOD at 18 mo
3	*EWSR1-CREB1*	33/M	Ileum	Epithelioid	Pseudopapillary, pseudoalveolar	+	+++	+++	−	+	+	−	AWD at 1.5 mo
4	*EWSR1-ATF1*	50/F	Stomach	Epithelioid	Solid sheets, nests	−	+	+++	+	−	−	−	AWD at 24 mo
5	*EWSR1* (+++)	20/F	SI	Spindled	Fascicular, nests	−	+++	+++	−	+	++	−	NED at 20 mo
6	All Negative	52/M	Ileum	Epithelioid	Solid sheets, nests	+	+++	+++	++	NP	−	++	DOD at 22 mo
7	*EWSR1*- (unknown partner)	46/M	Stomach	Epithelioid, oval	Solid sheets	+	+++	+++	−	NP	NP	−	No data
8	*EWSR1-ATF1*	34/F	Stomach	Epithelioid, spindled	Solid sheets, pseudoalveolar	+	+	+++	−	NP	NP	−	DOD at 19 mo
9	NP	37/F	Ileum	Epithelioid, oval	Solid sheets, nests	+	+++	NP	+	+	NP	NP	No data
10	*EWSR1-ATF1*	77/F	Colon	Epithelioid, spindled	Solid sheets, nests	+	+++	+++	+++	NP	−	+	DOD at 106 mo
11	Negative per report	31/M	Colon	Epithelioid, oval	Solid, microcystic	−	+++	NP	+++	NP	NP	NP	DOD at 3 mo
12	*EWSR1*-(unknown partner)	17/M	SI	Epithelioid, oval	Nests, infiltrative	+	+	+++	−	−	−	−	No data
13	*EWSR1-ATF1*	60/M	Ileum	Epithelioid, oval	Solid sheets, nests	−	+++	+++	++	−	NP	NP	AWD at 36 mo
14	*EWSR1-CREB1*	60/F	Jejunum	Epithelioid, spindled	Solid sheets, nests	−	+++	+++	−	+	NP	NP	NED at 41 mo
15	*EWSR1-CREB1*	56/M	Stomach	Epithelioid, oval	Solid sheets, nests	−	+++	+++	−	+++	NP	NP	No data
16	*EWSR1*-NP	28/F	SI	Epithelioid, oval	Solid sheets, nests	−	+++	+++	+++	NP	NP	+++	DOD at 23 mo

A/S indicates age/sex; AWD, alive with disease; DOD, dead of disease; NED, no evidence of disease; NP, not performed; OLGC, osteoclast-like giant cells; SI, small intestine.

TABLE 3.

Immunohistochemical and FISH Results for Cases of GNET

Antibody	1	2	3	4	5	6	7	8	9	10	11	12	13	14	15	16
Melanocytic																
S-100	+++	+++	+++	+	+++	+++	+++	+	+++	+++	+++	+	+++	+++	+++	+++
HMB45	−	−	−	−	−	−	−	−	NP	−	−	−	−	−	−	−
Melan A	−	−	−	−	−	−	−	−	NP	−	−	−	−	−	−	−
Tyros.	−	−	−	−	−	−	−	−	NP	−	−	−	−	−	−	NP
MITF	−	−	−	−	−	−	−	−	NP	−	NP	−	−	−	−	NP
GIST																
DOG-1	−	−	−	−	−	−	−	−	NP	−	NP	−	−	−	−	NP
CD34	−	−	−	−	−	−	−	−	−	NP	−	−	−	−	−	−
CD117	−	−	−	−	−	−	−	−	NP	−	−	−	−	−	−	−
Neural																
SOX10	+++	+++	+++	+++	+++	+++	+++	+++	NP	+++	NP	+++	+++	+++	+++	NP
Synaptophysin	++	+	−	+	−	++	−	−	+	+++	+++	−	++	−	−	+++
Chromogranin A	−	−	−	−	−	NP	NP	NP	−	−	NP	−	NP	NP	−	−
NFP	−	−	−	−	−	NP	NP	NP	+	NP	NP	−	NP	NP	NP	NP
CD56	+	+	+++	−	+	NP	NP	NP	+	NP	NP	−	−	+	+++	NP
CD99	−	−	−	−	−	NP	NP	NP	NP	NP	NP	−	NP	NP	NP	NP
NB84	+	+	+	−	++	−	NP	NP	NP	−	NP	−	NP	NP	NP	NP
NeuN	−	−	−	−	−	−	NP	NP	NP	−	NP	−	NP	NP	NP	NP
NSE-p	++	+	−	−	−	++	−	−	NP	+	NP	−	NP	NP	NP	+++
GFAP	−	−	−	−	−	NP	NP	NP	NP	NP	NP	−	NP	NP	NP	NP
Vimentin	+++	+++	+++	+++	+++	NP	NP	NP	+++	NP	+++	+++	+++	NP	+++	NP
SMA	−	−	−	−	−	−	−	−	−	NP	−	−	−	−	−	−
Desmin	−	−	−	−	−	−	−	−	−	NP	NP	−	−	−	−	−
AE1/AE3	−	−	−	−	−	NP	NP	NP	−	−	−	−	−	−	−	−
Cam 5.2	+	−	−	−	−	NP	NP	NP	NP	NP	NP	−	NP	−	NP	−
MIB-1	30.4	29.3	24.1	23.1	22.1	NP	NP	NP	NP	NP	NP	23.6	NP	NP	NP	NP
FISH																

Antibody	1	2	3	4	5	6	7	8	9	10	11	12	13	14	15	16
EWSR1	+	+	+	+	−	−	+	+	NP	+	NP	+	+	+	+	+
ATF1	+	+	−	+	−	−	−	+	NP	+	NP	−	+	−	−	NP
CREB1	−	−	+	−	−	−	−	−	NP	−	NP	−	−	+	+	NP
FUS	−	−	−	−	−	−	−	−	NP	−	NP	−	−	−	−	NP

DOG-1 indicates discovered on GIST 1; GFAP, glial fibrillary acidic protein; MITF, microphthalmia transcription factor; NeuN, NEUronal nuclei; NFP, neurofilament protein; NP, not performed; NSE-p, neuron-specific enolase, polyclonal; SMA, smooth muscle actin; +++, diffuse; ++, moderate; +, focal; +(bolded), positive break apart.

Am J Surg Pathol. Author manuscript; available in PMC 2020 September 09.

TABLE 4.

Ultrastructural Features of GNET

Case	Cell Shape	Processes	Junctions	Dense-core Granules	Intermediate Filaments	Microtubules	Other
1	Polygonal	Interdigitated	No evidence	+	No evidence	No evidence	Glycogen
2	Polygonal	Bulbous synaptic processes	No evidence	+	+	+	Synaptic vesicles
	Spindled	No evidence	Intermediate junctions	No evidence	No evidence	No evidence	Investment of basal lamina
3	Polygonal	Bulbous processes	No evidence	+	+	+	Synaptic vesicles
4	Polygonal	Interdigitated	No evidence	+	No evidence	No evidence	Glycogen
5	Polygonal	Interdigitated	Macula adherens	+	++	No evidence	

Am J Surg Pathol. Author manuscript; available in PMC 2020 September 09.